Missouri University of Science and Technology

Scholars' Mine

Physics Faculty Research & Creative Works   Physics

01 Jan 2007

Angular Distributions from Photoionization of H_2^+

J. Colgan

O. Al-Hagan

Jerry Peacher
Missouri University of Science and Technology, peacher@mst.edu

Don H. Madison
Missouri University of Science and Technology, madison@mst.edu

et. al. For a complete list of authors, see https://scholarsmine.mst.edu/phys_facwork/328

Angular distributions from photoionization of H_2^+

M. Foster[*] and J. Colgan

Theoretical Division, Los Alamos National Laboratory, Los Alamos, New Mexico 87545, USA

O. Al-Hagan, J. L. Peacher, and D. H. Madison[†]

*Physics Department and Laboratory for Atomic, Molecular, and Optical Research,
University of Missouri–Rolla, 1870 Miner Circle, Rolla, Missouri 65409, USA*

M. S. Pindzola[‡]

Department of Physics, Auburn University, Auburn, Alabama 36849, USA

A study is made of the differential cross sections arising from the photoionization of H_2^+. Previous studies indicated surprising differences in the shapes of the angular distributions calculated from exterior complex scaling and 2C methods. To further explore these differences, we have calculated the angular distributions from the photoionization of H_2^+ using an independent two-body Coulomb function (2C) method and a distorted wave approach. As a final test, we also present calculations using a time-dependent technique. Our results confirm the discrepancies found previously and we present possible reasons for these differences.

PACS number(s): 33.80.Eh, 33.80.Rv

I. INTRODUCTION

The hydrogen molecular ion, H_2^+, provides an ideal testing ground for developing theoretical techniques to treat molecular photoionization. For photoionization of H_2^+, the wave function can be calculated analytically in confocal elliptical coordinates for the initial and final states [1] which provides an important check for theories developed for more complicated molecular systems. Ideally, any theoretical method used to study multielectron molecules should be able to compute the photoionization of H_2^+ in a straightforward manner.

Recently, several theories have been proposed to examine molecular photoionization problems [2–6]. In initial calculations, two of these methods [the two-body Coulomb function (2C) technique [2] and the exterior complex scaling method (ECS) [3]] presented angular distributions for the single photoionization of H_2^+, and surprising differences were found between the results of the two methods for the shapes of the angular distributions of the ionized electron. The 2C technique uses products of Coulomb waves to describe the final molecular state, with appropriate correlation factors included to describe the final-state interactions. The ECS method was originally developed to examine electron and photon collisions with atoms [7] and computes the final state wave functions by rotating the outgoing wave into the complex plane, where it decays asymptotically. In this paper we investigate this discrepancy in the angular distributions of the ionized electron from H_2^+ in some detail. First, we use our own 2C method to compute the angular distributions for the photoionization of H_2^+ and also repeat our calculations using a distorted-wave approach. We also extend previous time-dependent calculations [4] to calculate the angular dif-

ferential cross sections for the photoionization of H_2^+ as a final check. For double photoionization of H_2, a time-dependent close-coupling technique has recently been shown to agree with ECS calculations for both total and angular differential cross sections [8,9]. Atomic units are used except where otherwise stated.

II. THEORY

The angular differential cross section in the dipole approximation using the velocity gauge is given by [10]

$$\frac{d\sigma}{d\Omega} = \frac{4\pi^2 \alpha k}{\omega}|T_{fi}^{e^-}|^2, \tag{1}$$

where α is the fine-structure constant, and ω is the photon frequency. In the Born-Oppenheimer approximation the dipole approximation matrix element using the velocity gauge is defined by

$$T_{fi}^{e^-} = \langle \psi_k | \hat{\epsilon} \cdot \vec{\nabla}_r | \psi_i \rangle, \tag{2}$$

where $\hat{\epsilon}$ is the direction of polarization. The electron momentum, $\vec{k}$, is relative to the molecular center of mass. In this paper, the dipole approximation matrix element is calculated in the velocity gauge as presented in Eq. (2). The matrix element is an integration only over the electronic coordinates. Figure 1 shows the molecular coordinates used in Eq. (2). For the initial state wave function, ψ_i, a linear combination of atomic orbitals (LCAO) wave function [11] is used. The LCAO wave function is given by

$$\psi_i = [2(1+S)]^{-1/2}(a+b), \tag{3}$$

where

*Electronic address: foster@lanl.gov
†Electronic address: madison@umr.edu
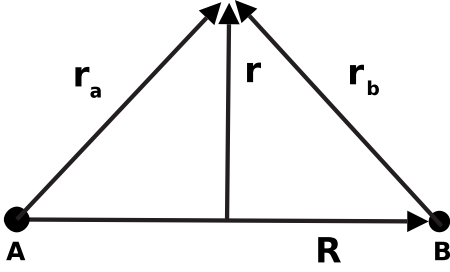‡Electronic address: pindzola@physics.auburn.edu

FIG. 1. Molecular coordinates: $\vec{R}$ is the relative vector of the two protons and $\vec{r}$ is the electron position with respect to the nuclear center of mass.

$$a = \sqrt{\frac{Z^3}{\pi}}e^{-Zr_a}, \quad b = \sqrt{\frac{Z^3}{\pi}}e^{-Zr_b}, \quad S = \langle a|b \rangle.$$

Here Z is the nuclear charge, and the relative electronic coordinates $\vec{r}_a$ and $\vec{r}_b$ are shown in Fig. 1.

A. Two-body Coulomb final-state wave function

For the final state wave function, ψ_k, a product of two 2Cs is inserted into Eq. (2). Each Coulomb distortion represents the two-body interaction between the ionized electron and one of the residual protons [2]. The 2C final-state wave function is defined by

$$\psi_k^{2C}(\vec{r}_a, \vec{r}_b) = (2\pi)^{-3/2}N\exp\left[i\frac{\vec{k}}{2}\cdot(\vec{r}_a + \vec{r}_b)\right]C(\vec{r}_a)C(\vec{r}_b),$$

(4)

where N is given by

$$N = e^{-\pi\alpha'/2}\Gamma(1 - i\alpha'),$$

(5)

where Γ is the gamma function and $\alpha' = -1/k$. The relative electronic coordinates, $\vec{r}_a$ and $\vec{r}_b$, are defined in Fig. 1. The Coulomb distortion factors in Eq. (4) are then given by

$$C(\vec{x}) = {}_1F_1(i\alpha', 1, -i(kx + \vec{k}\cdot\vec{x})),$$

(6)

where ${}_1F_1$ is a confluent hypergeometric function.

B. Distorted wave theory

In the distorted wave approach, the final-state wave function, ψ_k, for the ejected electron in Eq. (2) is replaced with a solution of the Schrödinger equation using a spherically symmetric potential to represent the ion

$$[\nabla_r^2 - 2U(r) + k^2]\chi_k = 0.$$

(7)

The spherically symmetric potential $U(r)$ is formed by averaging the molecule about the center of mass over all possible orientations. This is equivalent to placing a net charge of +2 on a spherical shell of radius unity. Consequently, the spherically symmetric potential, $U(r)$, is equivalent to the potential of a thin metal sphere of radius unity carrying a net charge of +2.

C. Time-dependent theory

The time-dependent method used to treat the single photoionization of H_2^+ has been presented in some detail previously [4]. The time-dependent method was recently extended to treat two electrons for the double photoionization of H_2 [8,9]. Here we briefly recap the time-dependent equations and show how the angular differential cross sections can be extracted in a straightforward manner.

By expanding the total wave function for the single electron using

$$\psi(r, \theta, \phi, t) = \sum_m \frac{P_m(r, \theta, t)}{r\sqrt{\sin\theta}}\frac{e^{im\phi}}{\sqrt{2\pi}},$$

(8)

we can write the time-dependent equation for photoionization of H_2^+ in the form

$$i\frac{\partial P_m(r, \theta, t)}{\partial t} = T_m(r, \theta)P_m(r, \theta, t) + V_m(r, \theta)P_m(r, \theta, t)$$
$$+ W_m(r, \theta, t)P_m(r, \theta, t).$$

(9)

Here $T_m(r, \theta)$ contains kinetic energy operators and $V_m(r, \theta)$ contains nuclear and centrifugal terms [4]. The interaction with the field is represented by $W_m(r, \theta, t)$, which is given by

$$W_m(r, \theta, t) = E(t)\cos(\omega t)r\cos\theta\delta_{m,0}$$

(10)

when the field is oriented parallel to the internuclear axis, and

$$W_m(r, \theta, t) = \frac{1}{2}E(t)\cos(\omega t)r\sin\theta(\delta_{m,1} + \delta_{m,-1})$$

(11)

when the field is oriented perpendicular to the internuclear axis. After propagation of the time-dependent equation for between 10 and 15 periods to some time T, the total cross section [4] for single photoionization can be written as

$$\sigma_m = \frac{\omega}{I}\frac{1}{T}\sum_l \int dk|\bar{P}_l^m(k, T)|^2,$$

(12)

where I is the incident intensity and

$$\bar{P}_l^m(k, T) = \int dr \int d\theta R_{klm}^*(r, \theta)P_m(r, \theta, T).$$

(13)

Here $R_{klm}(r, \theta)$ are H_2^+ distorted waves [9]. In the time-dependent calculations presented here, all orbital angular momenta up to $l = 7$ were retained in the sum in Eq. (12).

The angular differential cross section for photoionization of H_2^+ is then expressed as

$$\frac{d\sigma}{d\Omega} = \frac{\omega}{I}\frac{1}{T}\int dk\left|\sum_l(-i)^l e^{i\sigma_l}\left\{\bar{P}_l^{m=0}(k, T)Y_{l0}(\theta, \phi)\cos\theta_N\right.\right.$$
$$+ \bar{P}_l^{m=1}(k, T)Y_{l1}(\theta, \phi)\sin\theta_N\left[\frac{\cos\phi_N - i\sin\phi_N}{\sqrt{2}}\right]$$
$$\left.\left.+ \bar{P}_l^{m=-1}(k, T)Y_{l-1}(\theta, \phi)\sin\theta_N\left[\frac{\cos\phi_N + i\sin\phi_N}{\sqrt{2}}\right]\right\}\right|^2,$$

(14)

with (θ_N, ϕ_N) the angles between the molecule and the polarization direction, and σ_l is the Coulomb phase shift. Equation (14) is then given in units of a_0^2/sr.

D. Atomic limit

As the internuclear distance, $R \rightarrow 0$, all photoionization theories should recover the differential cross sections for photoionization of He$^+$. Photoionization of He$^+$ is a two-body process with a known wave function for He$^+$. The final-state wave function in the atomic limit is Eq. (7) with $U(r)$ as a Coulomb potential. The spherically symmetric potential used in the distorted wave theory, $U(r) \rightarrow -\frac{2}{r}$ as $R \rightarrow 0$. Consequently, the distorted wave theory properly recovers the correct atomic limit cross sections. In the atomic limit, since the two-body wave functions are exact, the dipole matrix element, Eq. (2), is invariant with respect to gauge, i.e., length, velocity, or acceleration.

However, in the atomic limit, the 2C theory does not recover the photoionization of the He$^+$ cross section. In the limit that the internuclear distance, $R \rightarrow 0$, $r_a = r_b = r$. Then the 2C wave function in Eq. (4) becomes

$$\psi_{\vec{k}}^{2C}(r, R=0) = (2\pi)^{-3/2} N \exp[i\vec{k} \cdot \vec{r}] C(r)^2. \quad (15)$$

Equation (15) has a similar form to the exact result, but the normalization, N, and the argument, α', in the Coulomb distortion factor are not correct. Also, the Coulomb distortion is squared leading to the improper absolute magnitude of the differential cross section in the atomic limit. The 2C wave function is also not gauge invariant due to the incorrect argument in the confluent hypergeometric function. For the time-dependent method, the atomic limit is always recovered. Also, the time dependent method is gauge invariant for both the atomic limit and for the photoionization of the molecular ion. The gauge invariance is broken in the distorted wave method for the molecular ion.

III. RESULTS

In Fig. 2, the comparison between the 2C and ECS results as presented previously [3] is shown. Angular distributions are presented at polarization angles of $\theta_N = 0°$, 30°, 60°, and 90° with respect to the molecular axis. The ionized electron ($E_e = 10$ eV) is ejected into the plane defined by the polarization and molecular axes. The magnitudes of the original 2C results are unavailable. Thus Fig. 2 compares only the shape of the angular distributions. The ECS angular distributions (solid curve) in Fig. 2 are quite different in shape from those calculated using the 2C method (dashed curve).

We present absolute angular differential cross sections for photoionization of H$_2^+$ at the same polarization angles of $\theta_N = 0°$, 30°, 60°, and 90° in Fig. 3. The ECS theory is compared to the time-dependent method as described previously. The two calculations are in good agreement for all the polarization angles with only some differences in the magnitudes of the angular distributions around $\theta = 90°$. The time-dependent and ECS calculations provide a benchmark for determining the magnitudes and shapes of the differential cross sections for photoionization of H$_2^+$. Previous compari-
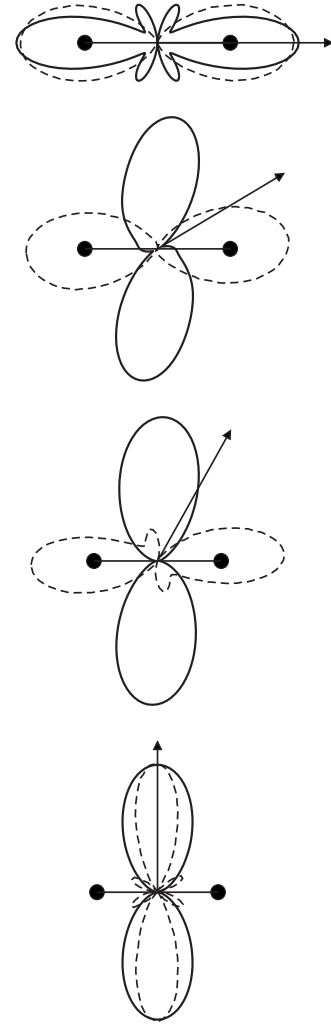

FIG. 2. Angular distributions for H$_2^+$ at polarization angles $\theta_N = 0°$, 30°, 60°, and 90° (top to bottom) with respect to the molecular axis (horizontal). The ionized electron is ejected in the plane of polarization and molecular axis and has $E_e = 10$ eV. Solid curve: ECS results from [3], and the dashed curve: 2C angular distributions of Ref. [2].

sons between ECS and the time-dependent methods for other atomic and molecular systems have shown similar agreement [9,12].

Figure 4 shows the ECS results versus the 2C results independently carried out by the authors of this paper. The 2C angular distributions presented in Fig. 4 are similar in shape to the 2C results calculated in Ref. [2]. The 2C results in Fig. 4 show significant magnitude discrepancies relative to the ECS results. The 2C theory has been reduced by scaling factors of 100, 10, and 2 for polarization angles $\theta_N = 0°$, 30°, and 60°, respectively. The large magnitude discrepancy between the 2C method and ECS theory is not surprising, since magnitude discrepancies have been previously observed between 2C methods and experimental measurements for double photoionization of helium [13]. The angular distributions calculated by the 2C theory for all θ_N have distinctly different structures than the ECS results. For $\theta_N = 30°$ and 60°, the 2C theory peaks approximately 90° out of phase from the ECS results.
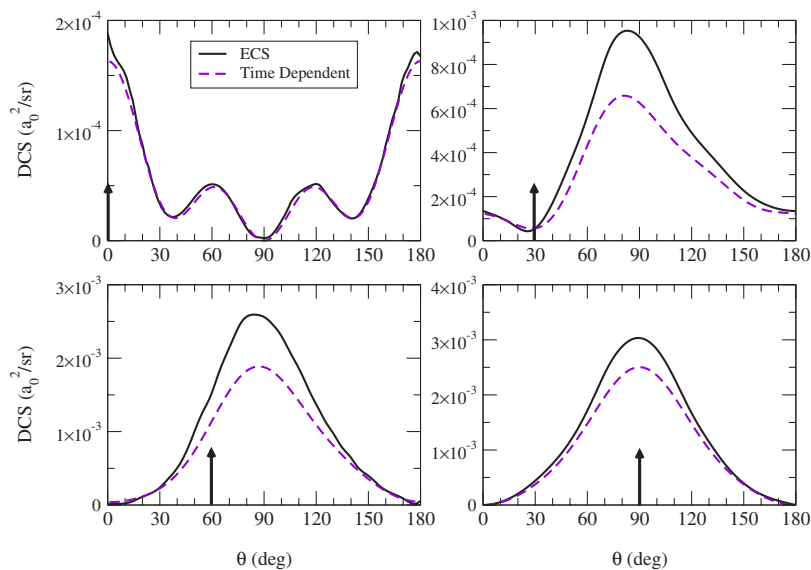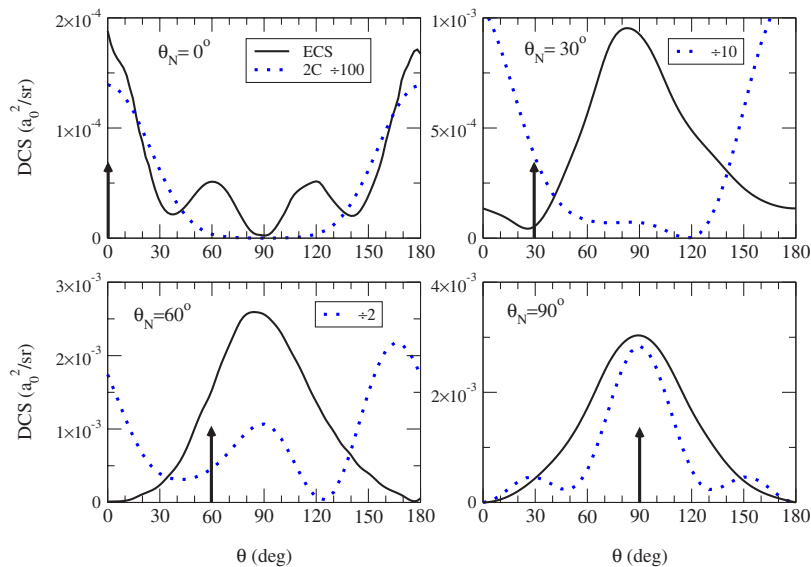
FIG. 3. (Color online) Differential cross section of photoionization of H_2^+ for an ionized electron $E_e = 10$ eV. The arrow represents the angle of polarization, θ_N. Solid line: ECS results and dashed line: time-dependent results.

FIG. 4. (Color online) Differential cross section of photoionization of H_2^+ for an ionized electron $E_e = 10$ eV. The arrow represents the angle of polarization, θ_N. Solid line: ECS results and dotted line: 2C results.
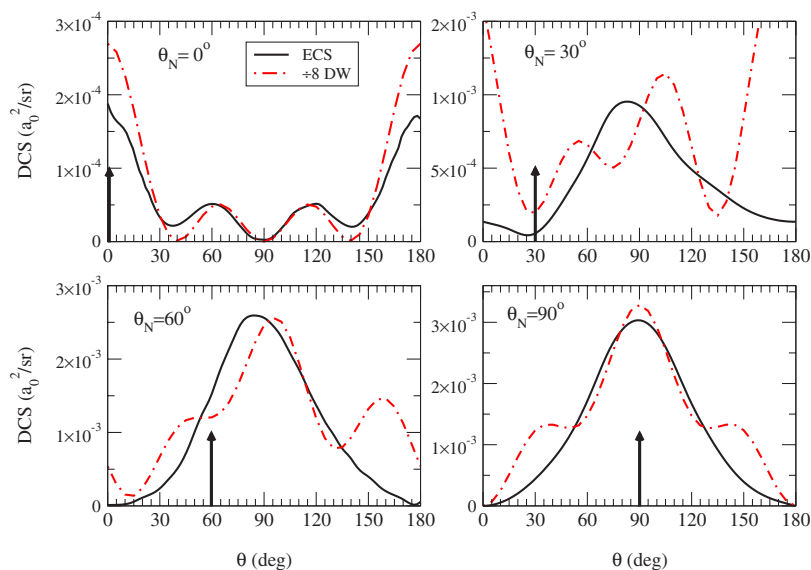

FIG. 5. (Color online) Differential cross section of photoionization of H_2^+ for an ionized electron $E_e = 10$ eV. The arrow represents the angle of polarization, θ_N. Solid line: ECS results and dashed-dotted line: distorted wave results.

The distorted wave treatment for photoionization of H_2^+ is shown as the dashed-dotted curve in Fig. 5. This simple technique has successfully predicted differential cross sections for electron impact ionization of various molecular systems [14–16]. The absolute magnitudes presented in Fig. 5 for the distorted wave treatment are significantly closer to the ECS results than the 2C calculations. The only scaling factor used to compare the distorted wave calculation to the ECS results was for $\theta_N = 0°$. The angular distributions calculated by the distorted wave method are in better agreement with the ECS results for all the polarization angles. The distorted wave method does not exactly predict the differential cross sections but provides more reasonable results than the 2C theory. Evidently, the distorted wave potential with the nuclei on a spherical shell appears to represent the actual molecular potential better than is contained in the 2C wave function despite of the fact that the 2C wave function depends on the orientation of the molecule whereas the final-state distorted wave does not. The distorted wave calculation gives a more accurate total cross section than the 2C approach because of the closer agreement in absolute magnitudes of the angular differential cross sections. Walter and Briggs [17] showed that the 2C angular distributions reach the simple plane wave limit for high enough electron energies. We have numerically observed that if the energy of the ionized electron is large (keV range) the 2C and distorted wave calculations also converge.

IV. SUMMARY

In summary, we have reproduced the original calculations for photoionization of H_2^+ performed by Refs. [2,3]. Our exact time-dependent calculation gave results similar to the ECS differential cross sections. The 2C calculations shown here agree with the original 2C results of Ref. [2]. However, the 2C theory is less than satisfactory when compared to the absolute differential cross sections from the ECS or time-dependent calculations and the 2C approach does not tend to the correct atomic limit. A distorted wave treatment of the ionized electron in the field of the two residual protons was also presented. The distorted wave differential cross sections provided more reasonable results for both the absolute magnitudes and angular distributions.

ACKNOWLEDGMENTS

[1] D. R. Bates, K. Ledsham, and P. L. Stewart, Proc. R. Soc. London, Ser. A **246**, 28 (1953).

[2] M. Walter and J. Briggs, J. Phys. B **32**, 2487 (1999).

[3] T. N. Rescigno, D. A. Horner, F. L. Yip, and C. W. McCurdy, Phys. Rev. A **72**, 052709 (2005).

[4] J. Colgan, M. S. Pindzola, and F. Robicheaux, Phys. Rev. A **68**, 063413 (2003).

[5] W. Vanroose, F. Martín, T. N. Rescigno, and C. W. McCurdy, Phys. Rev. A **70**, 050703(R) (2004).

[6] A. S. Kheifets and Igor Bray, Phys. Rev. A **72**, 022703 (2005).

[7] C. W. McCurdy, M. Baertschy, and T. N. Rescigno, J. Phys. B **37**, R137 (2006).

[8] J. Colgan, M. S. Pindzola, and F. Robicheaux, J. Phys. B **37**, L377 (2004).

[9] J. Colgan, M. S. Pindzola, and F. Robicheaux, Phys. Rev. Lett. **98**, 153001 (2007).

[10] B. H. Bransden and C. J. Joachain, *Physics of Atoms and Molecules*, 2nd ed. (Pearson Education Limited, Harlow, 2003), Chap. 13, p. 748.

[11] H. D. Cohen and U. Fano, Phys. Rev. **150**, 30 (1966).

[12] D. A. Horner, J. Colgan, F. Martín, C. W. McCurdy, M. S. Pindzola, and T. N. Rescigno, Phys. Rev. A **70**, 064701 (2004).

[13] S. Otranto and C. R. Garibotti, Phys. Rev. A **67**, 064701 (2003).

[14] Junfang Gao, D. H. Madison, and J. L. Peacher, J. Phys. B **39**, 1275 (2006).

[15] D. S. Milne-Brownlie, M. Foster, Junfang Gao, B. Lohmann, and D. H. Madison, Phys. Rev. Lett. **96**, 233201 (2006).

[16] J. Gao, D. H. Madison, and J. L. Peacher, Phys. Rev. A **72**, 020701(R) (2005).

[17] M. Walter and J. Briggs, Phys. Essays **13**, 297 (2000).